ARTICLES

The cohesin ring concatenates sister DNA molecules

Christian H. Haering[1]*†, Ana-Maria Farcas[1]*, Prakash Arumugam[1]†, Jean Metson[1] & Kim Nasmyth[1]

Sister chromatid cohesion, which is essential for mitosis, is mediated by a multi-subunit protein complex called cohesin. Cohesin's Scc1, Smc1 and Smc3 subunits form a tripartite ring structure, and it has been proposed that cohesin holds sister DNA molecules together by trapping them inside its ring. To test this, we used site-specific crosslinking to create chemical connections at the three interfaces between the three constituent polypeptides of the ring, thereby creating covalently closed cohesin rings. As predicted by the ring entrapment model, this procedure produced dimeric DNA–cohesin structures that are resistant to protein denaturation. We conclude that cohesin rings concatenate individual sister minichromosome DNA molecules.

Sister chromatid cohesion is mediated by a multi-subunit complex called cohesin which contains four core subunits: Smc1 and Smc3, which are members of the structural maintenance of chromosomes (SMC) protein family, and two non-SMC subunits, Scc1 (also called Mcd1) which is a member of the kleisin family, and Scc3 (SA)[1,2]. Sister chromatid disjunction occurs when all chromosomes have been bi-oriented, and it is triggered by site-specific cleavage of the Scc1 subunit of cohesin by separase[3]. The Smc1 and Smc3 subunits of cohesin both form rod-shaped molecules that heterodimerize by means of 'hinge' domains situated at the ends of 30-nm-long intramolecular antiparallel coiled coils[4,5]. ATPase 'heads' at the other ends are connected by the Scc1 kleisin subunit of cohesin, thereby forming a tripartite ring with a 35 nm diameter[4,6]. It has been proposed that cohesin holds sister chromatids together by trapping sister DNAs inside its ring. By severing Scc1, separase is thought to open the ring and thereby release sister DNAs from their topological embrace.

To investigate the physical nature of sister chromatid cohesion, we recently used sucrose gradient sedimentation and gel electrophoresis to purify cohesed (held together by cohesin) sister chromatids of small circular minichromosomes from yeast[7]. The minichromosome dimers are composed of individual DNAs packaged into nucleosomes that are converted to monomers by cleaving Scc1 or by linearizing their DNA. Notably, their formation depends on centromeres as well as cohesin (see Supplementary Information and Supplementary Fig. 1). These data are consistent with (but do not prove) the notion that cohesin attaches to chromatin using a topological mechanism. However, they do not exclude the possibility that cohesion requires the non-topological association of cohesin rings bound to different chromatin fibres[8]. If cohesin holds dimeric minichromosomes together by trapping them inside its ring, then introducing covalent connections between the Smc1–Smc3 hinge, Smc1 head–Scc1-carboxy terminal and Smc3 head–Scc1-amino terminal interfaces should create a chemically circularized cohesin ring within which sister DNAs would be trapped even after protein denaturation (Fig. 1a). We describe here experiments that test this prediction.

Covalent connection of the three cohesin ring subunits

To connect cohesin subunit interfaces covalently, we used the homobifunctional thiol-reactive chemicals dibromobimane (bBBr) and bis-maleimidoethane (BMOE) which bridge thiol groups up to 5 Å or 8 Å respectively[9,10] (Supplementary Fig. 2). We created a homology model of the yeast Smc1–Smc3 hinge heterodimer based on the homodimeric *Thermotoga maritima* crystal structure[4,11] and identified two juxtaposed side chains that we mutated to cysteines. Incubation of the engineered Smc1–Smc3 hinge dimer with either bBBr or BMOE caused efficient crosslinking within a few minutes (Fig. 1b). Notably, crosslinking was dependent on both cysteine substitutions. We used the same approach to connect the loop between the two β-strands of the winged-helix of Scc1 to a β-strand in the ATPase head of Smc1 (ref. 12; Fig. 1c). Because no structural information is available for the interface between the ATPase head of Smc3 and the amino-terminal domain of Scc1, we expressed Smc3 and Scc1 as a fusion protein, using a long flexible linker containing triple target sequences for the TEV protease to connect the C terminus of Smc3 with the N terminus of Scc1 (Smc3–TEV–Scc1)[13]. To create cohesin rings that could be chemically circularized by BMOE or bBBr, the cysteine substitutions were introduced into both Smc3–TEV–Scc1 and Smc1.

Crosslinking produces SDS-resistant minichromosome dimers

A 2.3-kilobase (kb) circular minichromosome[7] was introduced into yeast strains in which the Smc1 and Smc3–TEV–Scc1 polypeptides contained either all four cysteine substitutions or only a subset of these. After nocodazole arrest and cell lysis, extracts were centrifuged through sucrose gradients, and fractions containing monomeric and dimeric minichromosomes were detected by native agarose gel electrophoresis and Southern blotting. Dimeric minichromosomes could still be isolated from yeast cells in which the cohesin ring subunits had been engineered to permit cohesin circularization. The cysteine substitutions had little adverse effect, but the fusion of Scc1 to Smc3 roughly halved the fraction of dimeric minichromosomes (Fig. 2a). This was not surprising as the fusion causes partial cohesion defects *in vivo*[13]. Dithiothreitol (DTT), sucrose and other low-molecular-mass contaminants were removed from the gradient fractions by dialysis and cohesin subunits were treated with bBBr, BMOE or merely dimethylsulphoxide (DMSO) solvent. After quenching the reaction by the re-addition of DTT, SDS was added to a final concentration of 1% and the samples were heated to

[1]University of Oxford, Department of Biochemistry, South Parks Road, Oxford OX1 3QU, UK. †Present addresses: European Molecular Biology Laboratory (EMBL), Meyerhofstraße 1, 69117 Heidelberg, Germany (C.H.H.); Department of Biological Sciences, University of Warwick, Gibbet Hill Road, Coventry CV4 7AL, UK (P.A.).
*These authors contributed equally to this work.

65 °C for 4 min. The denatured samples were finally electrophoresed in agarose gels containing ethidium bromide, and minichromosome DNA was detected by Southern blotting.

Dimer fractions from control cells expressing unmodified cohesin contained four species of DNA (Fig. 2b, panel F). The fastest migrating and most predominant are supercoiled monomers (species 1; Fig. 2f). Owing to SDS in the loading buffer, the next two species (2 and 3) were poorly resolved from each other. These DNAs co-migrated with monomeric nicked circles produced by nicking enzyme after removal of nucleosomes with 2 M potassium chloride (Fig. 2d) and with (infrequently) intertwined—that is, concatenated—supercoiled DNAs isolated from a topoisomerase II mutant (Fig. 2e), and therefore include both of these species of DNA. The nicking enzyme treatment revealed that about 10% of DNAs from dimer (but not monomer) fractions are DNA–DNA concatemers (Fig. 2d and data not shown). The least abundant species (4) migrated more slowly than two intertwined supercoiled circles (3) but more rapidly than two intertwined nicked circles generated by treatment with nicking enzyme (5). We conclude that these DNAs

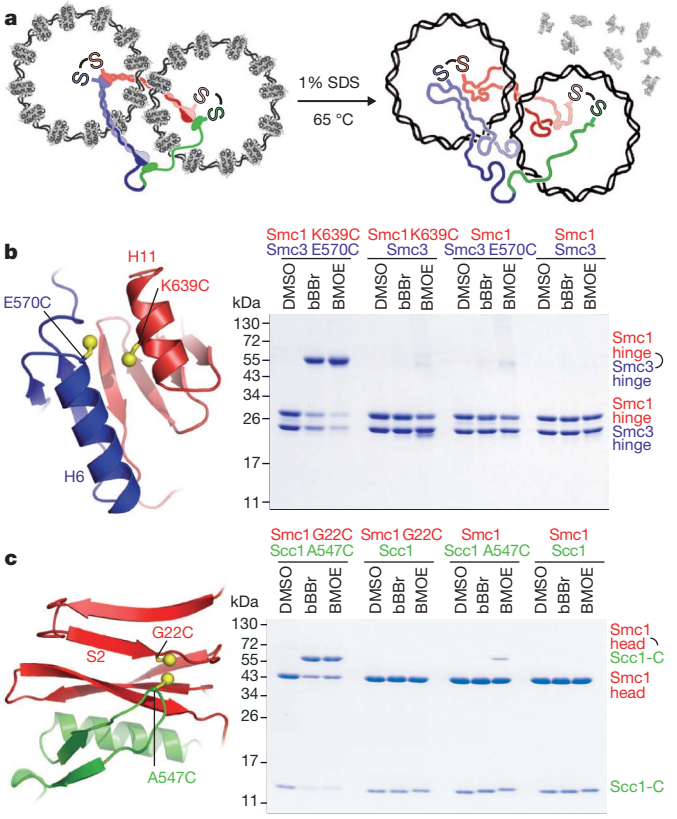

Figure 1 | Making covalently closed cohesin rings. **a**, Fusion of the C terminus of Smc3 with the N terminus of Scc1 and chemical crosslinking of engineered cysteine residues at the Smc1–Smc3 and Smc1–Scc1 interfaces creates a covalently closed cohesin ring. **b**, A homology model of the Smc1–Smc3 hinge interface using the homodimeric bacterial structure (Protein Data Bank (PDB) 1GXL) identifies two juxtaposed Cβ atoms in helix H11 of Smc1 and helix H6 of Smc3 at a distance compatible with crosslinking when mutated to cysteine. A Coomassie stained SDS–PAGE of wild-type and cysteine mutant yeast Smc1–Smc3 hinge domain dimers is shown. **c**, The structure of the yeast Scc1 C terminus bound to the head domain of Smc1 (PDB 1W1W) identifies two juxtaposed side chains that should allow crosslinking when mutated to cysteine. Complexes of wild-type and cysteine mutant yeast Smc1 head domain bound to the C-terminal domain of Scc1 resolved by SDS–PAGE are shown. The low-level crosslinking observed for the Smc1–Scc1(A547C) combination probably results from a reaction of BMOE with the engineered cysteine in Scc1 and the nearby ε-amino group of Smc1's lysine residue K20.

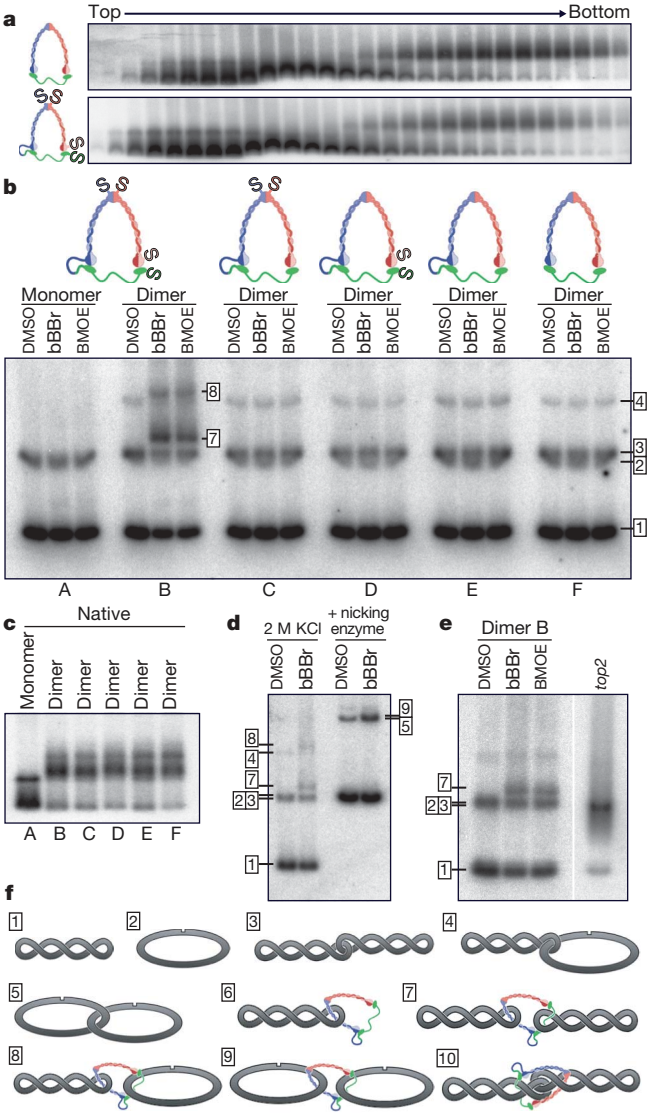

Figure 2 | Covalent cohesin circularization creates SDS-resistant minichromosome DNA dimers. **a**, Extracts from yeast strains harbouring the minichromosome and expressing wild-type cohesin (top) or Smc3–TEV–Scc1 and Smc1 containing the engineered cysteine pairs (bottom) were separated by gradient centrifugation. Minichromosome dimers sediment faster but electrophorese slower than monomers. **b**, Minichromosome monomer or dimer gradient fractions from yeast strains in which all three (K14856; panels A and B), two (K14857, K14859; panels C and D), one (K14858; panel E) or no (K14860; panel F) ring subunit interface(s) can be covalently linked were treated with DMSO, bBBr or BMOE and separated after denaturation. Monomer and dimer fractions contain supercoiled (1) and nicked (2) monomeric minichromosomes. Dimer fractions also contain supercoiled–supercoiled (3) and supercoiled–nicked (4) concatenated minichromosome DNAs. Only samples in which all three cohesin ring subunit interfaces have been covalently linked contain additional slower migrating bands, presumably corresponding to supercoiled–supercoiled (7) and supercoiled–nicked (8) cohesed minichromosomes. **c**, Input fractions for crosslinking reactions A–F run without denaturation. **d**, Treatment of non-crosslinked or crosslinked minichromosomes with nicking enzyme, after removal of nucleosomes by high salt, converts supercoiled (1), supercoiled–supercoiled (3, 7) or supercoiled–nicked (4, 8) minichromosomes to nicked (2) or nicked–nicked (5, 9) forms. **e**, A gradient dimer fraction from a topoisomerase II mutant strain (K15029) grown at the restrictive temperature was denatured. Concatenated minichromosomes (short exposure) co-migrate with bands (2) and (3) of K14856 (long exposure) on the same gel. **f**, Schemata of minichromosome conformations.

correspond to one supercoiled circle intertwined with one nicked circle.

Treatment of dimer fractions with bBBr or BMOE had no effect on the electrophoresis profile of minichromosome DNAs (Fig. 2b, panel F). Moreover, the very same pattern was observed when dimeric minichromosomes were isolated from strains expressing the Smc3–TEV–Scc1 fusion (Fig. 2b, panel E) and crosslinkable cysteine pairs at either the Smc1–Scc1 or the Smc1–Smc3 interface (Fig. 2b, panels C and D). In contrast, bBBr and BMOE but not DMSO alone caused the appearance of two additional species of DNA when dimers were isolated from a strain containing the Smc3–TEV–Scc1 fusion and cysteine pairs at both interfaces (Fig. 2b, panel B). The more abundant DNA species (7) migrated slightly more slowly than intertwined supercoiled circles, whereas the less abundant (8) migrated slightly more slowly than supercoiled circles intertwined with nicked circles. Their electrophoretic mobilities and the fact that neither was detected when identical crosslinking reactions were conducted with monomer fractions (Fig. 2b, panel A and Fig. 2c) suggest that they represent novel dimeric forms. Their formation occurs at the expense of supercoiled and nicked monomeric circles.

Our data suggest that the faster form (7) is a dimer of supercoiled monomeric circles associated with cohesin whereas the slower form (8) is a dimer between supercoiled and nicked circles associated with cohesin. Consistent with this, both were converted to a form (9) that co-migrates with intertwined nicked circles (5) when treated with nicking enzyme (Fig. 2d). The extra mass of cohesin probably has little effect on the electrophoretic mobility of this slow running species. Notably, neither novel dimer was produced when just one of the four cysteine substitutions was lacking (Supplementary Fig. 3a), suggesting that they arise due to the simultaneous crosslinking of both cysteine pairs at the Smc1–Smc3 hinge and Smc1–Scc1 interfaces. Crosslinked dimers were also produced when minichromosomes were isolated from cycling cultures (Supplementary Fig. 3a), suggesting that their formation is not an artefact caused by arresting cells with nocodazole. Finally, no slower migrating species could be observed when DNA was linearized with a restriction enzyme after crosslinking (Supplementary Fig. 3b). In conclusion, covalent closure of the cohesin ring converts dimeric but not monomeric minichromosomes to a dimeric form that is resistant both to SDS and to 2 M potassium chloride (native dimers are converted to monomers at 0.5–1 M potassium chloride; Supplementary Fig. 4).

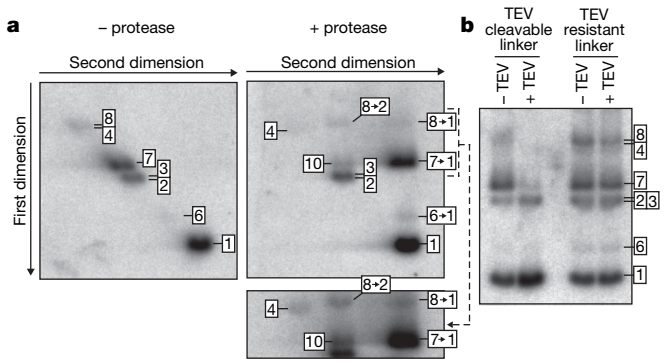

Figure 3 | Covalent circularization of cohesin holds individual DNAs together. a, Crosslinked and denatured samples were run on an agarose gel, excised and run on a second agarose gel in perpendicular direction. A thin slot between the first dimension lane and the second gel was filled with either agarose or agarose containing 0.2 mg ml^{-1} proteinase K. In the absence of protease, all bands run on a diagonal. In the presence of protease, supercoiled–supercoiled cohesed dimers (7) run as supercoiled monomers (7→1) in the second dimension, whereas supercoiled–nicked cohesed dimers (8) split up into supercoiled (8→1) and nicked (8→2) monomers in the second dimension, more clearly visible in a longer exposure (bottom panel). A faint band, presumably corresponding to cohesin bound supercoiled monomers (6), is converted into naked supercoiled monomers (6→1) on protease cleavage. An additional band (10) running off the diagonal presumably corresponds to supercoiled–supercoiled concatenated minichromosomes that had bound cohesin. **b**, Crosslinked minichromosome samples were treated with or without TEV protease before denaturation. The slower migrating bands (7 and 8) corresponding to cohesed minichromosomes disappear on TEV incubation if the Smc3–Scc1 linker contains triple target sequences for the protease (TEV-cleavable), but not if the −1 sites of the triple target sequence are mutated to lysine (TEV-resistant).

Circularized cohesin holds individual DNAs together

To test whether the SDS-resistant dimers produced by cohesin circularization are indeed monomeric DNAs held together by cohesin, we used two-dimensional gel electrophoresis. Denatured crosslinked samples were resolved on an agarose gel as before (the first dimension), and then electrophoresed perpendicularly through a thin zone of agarose or agarose containing proteinase K into a second agarose gel (the second dimension). Proteinase K should digest any proteins before DNAs enter the second gel and DNAs that ran as dimers in the first dimension should run as monomers in the second dimension if they were initially held together by a proteinaceous (that is, cohesin) connection. In the absence of proteinase K, all DNA species migrate identically in first and second dimensions and therefore lie on a diagonal line (Fig. 3a). Several species also ran on the diagonal in the presence of proteinase K, namely monomeric supercoils (1), monomeric nicked circles (2), intertwined supercoils (3), and nicked circles intertwined with supercoils (4) (Fig. 3a). In contrast, DNAs of presumptive dimers of two supercoiled minichromosomes held together by cohesin (7) migrated as monomeric supercoils in the second dimension (7→1), whereas presumptive supercoiled–nicked circle dimers held together by cohesin (8) split into monomeric supercoils (8→1) and nicked circles (8→2). Thus, chemical circularization of cohesin associated with native dimeric minichromosomes is accompanied by the crosslinking of monomeric DNAs to create SDS-resistant but protease-sensitive dimers.

The protease-containing two-dimensional gel revealed two new types of low abundance DNAs. The first (6) migrated considerably slower than monomeric supercoils in the first dimension but ran as monomeric supercoils in the second dimension (6→1). These DNAs were only detected in monomeric or dimeric minichromosome preparations in which cohesin rings had been covalently closed (data not shown). They presumably correspond to rare supercoiled monomers the migration of which is retarded by their association with (entrapment by) a chemically circularized cohesin ring. The second species (10) co-migrated with cohesin-mediated supercoiled dimers in the first dimension but with intertwined supercoils (and nicked circles) in the second dimension. These DNAs could correspond either to monomeric nicked circles associated with cohesin or, more probably, to intertwined supercoils that are also associated with cohesin.

If cohesin circularization by bBBr and BMOE crosslinking *per se* is responsible for the formation of SDS-resistant minichromosome dimers, then cleavage of the cohesin ring should be sufficient to release the monomeric DNAs. To test this, we incubated crosslinked dimeric minichromosome preparations with or without TEV protease to cleave the linker connecting Smc3 and Scc1. The presence of TEV greatly reduced both types of DNA dimers induced by the circularization of cohesin (7 and 8), which was accompanied by a corresponding increase in monomeric DNAs (1 and 2) (Fig. 3b). This effect was clearly caused by cleavage of the TEV sites in the Smc3–Scc1 linker because DNA dimers produced by circularization of cohesin with a TEV-resistant Smc3–Scc1 linker were unaffected by TEV protease (Fig. 3b). We conclude that the SDS-resistant association of sister DNAs induced by crosslinking the three subunits of cohesin does not merely accompany the circularization of cohesin but actually depends on it.

Cohesion by single or double cohesin rings?

The simplest explanation for the crosslinking results is that sister DNAs are topologically trapped within single (monomeric) cohesin rings (Supplementary Fig. 5a). An alternative albeit more complicated possibility envisions entrapment of sister DNAs either by rings that are themselves topologically intertwined (Supplementary Fig. 5b) or by dimeric cohesin rings. Only two cysteine crosslinks are needed for entrapment by single rings, whereas four are required by double ring models. If we knew the efficiency with which bBBr and BMOE crosslink the Smc1–Smc3 and Smc1–Scc1 interfaces and the number of cohesin bridges, then we could calculate the fraction of DNAs that should be trapped as dimers according to the two models and compare these to what is actually observed.

To estimate the protein crosslinking efficiency, we added purified Smc1–Smc3 hinge or Smc1 head–Scc1-C to crosslinkable minichromosome dimer preparations before crosslinking with bBBr or BMOE and denaturation. One-half of the reaction was run on SDS–PAGE and the fraction of crosslinked proteins was measured after SYPRO ruby staining (Fig. 4a). The other half was run on an agarose gel and the fraction of dimerized DNA was measured by Southern blotting (Fig. 4b). The fraction of rings expected to be crosslinked at both interfaces, which is given by multiplying individual crosslinking efficiencies, was 30% for both bBBr and BMOE. We would therefore expect 30% of DNAs to be dimerized if held together by a single cohesin ring but only 9% by a double ring. Estimating the actual number of bridges is harder because the gradient fractions contain much cohesin that is not associated with minichromosomes (data not shown). However, if we assume that a single bridge is sufficient to hold sister DNAs together and that cross-bridges form *in vivo* and survive fractionation *in vitro* with a defined probability (λ), then the fraction of chromosomes $f(x)$ with x bridges should fit a Poisson distribution. $f(0)$ can be measured directly, namely by measuring the fraction of monomeric minichromosomes (Supplementary Fig. 6a) and DNA–DNA concatemers (Fig. 2d), which permits calculation of λ (see Supplementary Information). Because $f(0)$ is large, most native dimeric minichromosomes are predicted to have a single bridge. Taking this into account, the single and double ring models predict 32% and 10% dimerization, respectively. The observed value with both reagents was 30% (Fig. 4b), which is inconsistent with the double ring model and close to that predicted by the single ring model.

Single and double ring models also make different predictions for heterozygous diploids that express equal amounts of TEV-cleavable and TEV-resistant Smc3–Scc1 fusion proteins (Supplementary Fig. 6b). In the case of one cross-bridge, the single ring model predicts that 50% of crosslinked dimers should survive cleavage of half the cohesin rings. In contrast, the double ring model predicts only 25% because cleavage of just one ring is sufficient to destroy dimers held together by intertwined rings. We isolated minichromosome dimers from cleavable and non-cleavable haploids, from a 1:1 mixture of the two and from heterozygous diploids. These were crosslinked, treated either with TEV protease or a non-catalytic TEV mutant, denatured with SDS and run on an agarose gel. The fraction of DNAs dimerized by crosslinking was measured by scanning Southern blots. This showed that about 50% of cohesed minichromosomes survived TEV treatment when isolated from heterozygous diploids as well as the 1:1 mixture of haploids (Fig. 4c). These data fit the single but not the double ring model. We note that the latter model also predicts that a sizeable fraction of crosslinked dimers (species 7 and 8) from heterozygous diploids should be converted by TEV cleavage to supercoiled monomers associated with cohesin (species 6), which is not observed (Fig. 4c).

Discussion

Our crosslinking experiments are consistent with the notion that sister minichromosome DNAs are entrapped by a single monomeric ring. Notably, they exclude the possibility that the connection between sister DNAs is mediated by non-topological interactions between cohesin complexes associated with each sister[8]. Given the specificity of the crosslinking by bBBr and BMOE, there is no reason to suppose that putative interactions between cohesin rings will have been crosslinked in our experiments. Double-ring models proposing topological cohesin–cohesin interactions or a gigantic ring formed by two cohesin complexes are difficult to reconcile with the findings that the fraction of DNAs dimerized is almost identical to the fraction of cohesin rings circularized and not to the square of this fraction, and that cleavage of half the cohesin rings reduces dimers to 50% and not 25%.

Our conclusion that sister chromatin fibres of dimeric minichromosomes are threaded through cohesin rings provides a simple and potentially adequate mechanism to explain the ability of cohesin to hold sister chromatids together. Cohesin could therefore be considered a 'concatenase'. It will be important to address whether it uses the same mechanism at loci farther away from core centromeres, whether it sometimes traps individual chromatin fibres, and if so whether it is capable of forming chromatin loops. We detected rare instances where the individual DNA trapping occurred on the minichromosomes, namely monomeric DNAs that on cohesin circularization are retarded in their electrophoretic mobility (species 6) in a

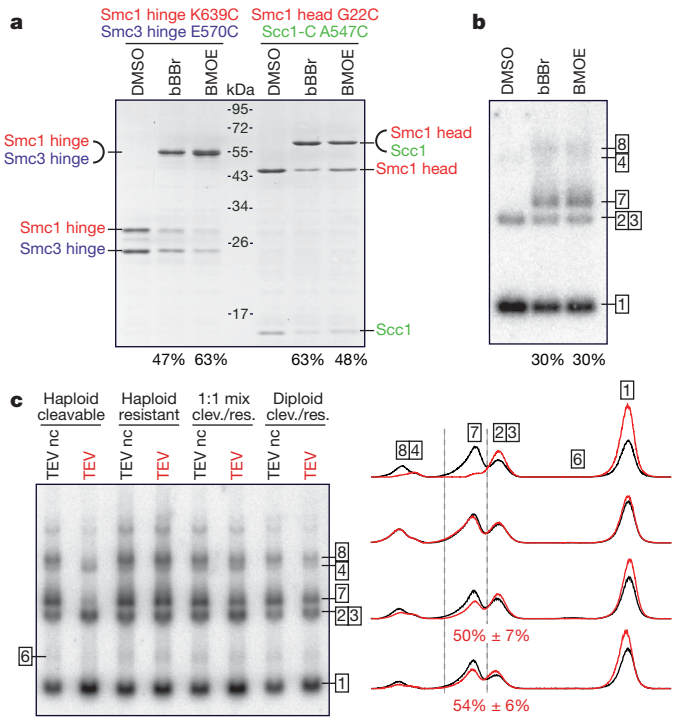

Figure 4 | Minichromosomes are cohesed by single cohesin rings. Protein–protein crosslinking efficiencies by bBBr and BMOE were measured by spiking dimer fractions (K14856) with purified double cysteine mutants of Smc1–Smc3 hinge or Smc1–Scc1-C complex preparations. **a**, After crosslinking, half the reactions were separated by SDS–PAGE and band intensities were measured after SYPRO Ruby staining. **b**, The remainder of the reactions was run on an agarose gel and the fractions of cohesed minichromosomes (7 + 8/total) were quantified after Southern blotting. **c**, Minichromosome dimer fractions from haploid strains expressing TEV-cleavable Smc3–Scc1 (K14856), from haploids expressing Smc3–Scc1 resistant to TEV cleavage (K15089), from a 1:1 mixture of the two haploids, or from a diploid strain containing one TEV-cleavable and one TEV-resistant *SMC3–SCC1* allele (K15267) were crosslinked with bBBr, treated with wild-type or a non-catalytic (nc; C151A) mutant of TEV protease, denatured and separated by agarose gel electrophoresis. Peaks corresponding to cohesed supercoiled minichromosome dimers (7) were integrated and the peak area after incubation with active versus non-catalytic TEV protease was compared. Assuming the number of cohesin cross-bridges follows a Poisson distribution, we would expect 53% or 27% of crosslinked dimers surviving TEV treatment for single or double ring models, respectively. The observed value is 54% ± 6% ($n = 3$; error ± s.d.); clev., cleavable; res., resistant.

manner that is destroyed by ring cleavage. Cohesin is known to associate with chromatin before DNA replication, when it cannot be involved in holding sisters together. Moreover, it can associate with replicated chromosomes in a way that does not lead to cohesion between sisters[12,14]. We suggest that cohesin frequently does trap individual chromatin fibres and that its activity in post-mitotic cells in Metazoa might involve this type of action[15,16]. If we are correct in concluding that cohesin is a novel type of concatenase, then it is not implausible to imagine that other SMC–kleisin complexes such as condensin and its bacterial equivalent have related activities. Indeed, the deep evolutionary roots of these types of complexes suggest that the ability to concatenate DNA may have been an activity without which DNA genomes could not have evolved.

METHODS SUMMARY

To establish cysteine crosslinking reactions, the Smc1 and Smc3 hinge domains were co-expressed in *Escherichia coli* and purified by means of a C-terminal His_6 tag on Smc1 and gel filtration. The Smc1 head–Scc1-C complex was co-expressed in insect cells using the baculovirus system and purified as described[12]. Proteins were incubated with DMSO or final concentrations of 200 μM bBBr or 1 mM BMOE before SDS–PAGE and Coomassie staining. Minichromosomes were isolated as described[7] following a slightly modified protocol. Gradient dimer fractions were dialysed against reaction buffer and incubated for 10 min with DMSO, 200 μM bBBr or 1 mM BMOE. Reactions were quenched by addition of DTT to 10 mM and proteins were denatured by 4 min incubation at 65 °C in 1% SDS before agarose gel electrophoresis and Southern blotting. Where indicated, quenched crosslinking reactions were incubated for 1 h at 30 °C with TEV protease at 0.2 mg ml^{-1}. To measure crosslinking efficiencies in minichromosome fractions, purified protein dimers were added at a final concentration of 3 μM to ensure saturated association of the nanomolar affinity interactions between the dimer subunits.

Full Methods and any associated references are available in the online version of the paper at www.nature.com/nature.

Received 5 December 2007; accepted 15 May 2008.
Published online 2 July 2008.

1. Nasmyth, K. & Haering, C. H. The structure and function of SMC and kleisin complexes. *Annu. Rev. Biochem.* **74,** 595–648 (2005).
2. Hirano, T. SMC proteins and chromosome mechanics: from bacteria to humans. *Phil. Trans. R. Soc. B* **360,** 507–514 (2005).
3. Uhlmann, F. *et al.* Cleavage of cohesin by the CD clan protease separin triggers anaphase in yeast. *Cell* **103,** 375–386 (2000).
4. Haering, C. H., Lowe, J., Hochwagen, A. & Nasmyth, K. Molecular architecture of SMC proteins and the yeast cohesin complex. *Mol. Cell* **9,** 773–788 (2002).
5. Hirano, M. & Hirano, T. Hinge-mediated dimerization of SMC protein is essential for its dynamic interaction with DNA. *EMBO J.* **21,** 5733–5744 (2002).
6. Gruber, S., Haering, C. H. & Nasmyth, K. Chromosomal cohesin forms a ring. *Cell* **112,** 765–777 (2003).
7. Ivanov, D. & Nasmyth, K. A physical assay for sister chromatid cohesion *in vitro*. *Mol. Cell* **27,** 300–310 (2007).
8. Milutinovich, M. & Koshland, D. E. Molecular biology. SMC complexes–wrapped up in controversy. *Science* **300,** 1101–1102 (2003).
9. Kim, J. S. & Raines, R. T. Dibromobimane as a fluorescent crosslinking reagent. *Anal. Biochem.* **225,** 174–176 (1995).
10. Dhar, G., Sanders, E. R. & Johnson, R. C. Architecture of the hin synaptic complex during recombination: the recombinase subunits translocate with the DNA strands. *Cell* **119,** 33–45 (2004).
11. Eswar, N. *et al.* Comparative protein structure modeling using Modeller. *Curr. Protoc. Bioinformatics* **Supplement 15,** 5.6.1–5.6.30, doi:10.1002/0471250953.bi0506s15 (2006).
12. Haering, C. H. *et al.* Structure and stability of cohesin's Smc1-kleisin interaction. *Mol. Cell* **15,** 951–964 (2004).
13. Gruber, S. *et al.* Evidence that loading of cohesin onto chromosomes involves opening of its SMC hinge. *Cell* **127,** 523–537 (2006).
14. Bausch, C. *et al.* Transcription alters chromosomal locations of cohesin in *Saccharomyces cerevisiae*. *Mol. Cell. Biol.* **27,** 8522–8532 (2007).
15. Schuldiner, O. *et al.* piggyBac-based mosaic screen identifies a postmitotic function for cohesin in regulating developmental axon pruning. *Dev. Cell* **14,** 227–238 (2008).
16. Pauli, A. *et al.* Cell-type-specific TEV protease cleavage reveals cohesin functions in *Drosophila* neurons. *Dev. Cell* **14,** 239–251 (2008).

Supplementary Information is linked to the online version of the paper at www.nature.com/nature.

Acknowledgements We thank S. Gruber for help with the design of cysteine mutations, and P. Fowler, D. Ivanov, V. Katis and all members of the Nasmyth laboratory for advice and discussions. This work was supported by the Medical Research Council, the Wellcome Trust and Cancer Research UK.

Author Information Reprints and permissions information is available at www.nature.com/reprints. Correspondence and requests for materials should be addressed to K.N. (kim.nasmyth@bioch.ox.ac.uk).

METHODS

Model of the *Saccharomyces cerevisiae* Smc1–Smc3 hinge structure. A structure model of the yeast Smc1–Smc3 hinge structure was created with the Modeller program[11] using an alignment of *S. cerevisiae* Smc1 amino acid residues 488–690 and Smc3 amino acid residues 496–699 with residues 475–679 of the *T. maritima* SMC protein and the coordinates of PDB accession code 1GXL.

Expression, purification and crosslinking of cohesin subunit domains. Sequences encoding amino acids 494–705 of the *S. cerevisiae* Smc3 hinge domain followed by an internal ribosome binding site and sequences encoding amino acids 486–696 of the *S. cerevisiae* Smc1 hinge domain fused to a C-terminal His_6 tag were cloned by PCR into the pET28 expression vector. Cysteine mutations were introduced by overlap extension PCR. The Smc1–Smc3 hinge domains were co-expressed in *E. coli* strain BL21(DE3)-RIPL (Stratagene) at 20 °C for 5 h after induction with 0.25 mM IPTG. Cells were lysed in 50 mM NaPi pH 8.0, 300 mM NaCl containing Complete EDTA free protease inhibitor mix (Roche) and the complex was purified using Ni^{2+}-chelating affinity chromatography followed by gel filtration on a Superdex 200pg 26/60 column (GE Healthcare) in TEN buffer (20 mM Tris-HCl pH 8.0, 1 mM EDTA, 1 mM NaN_3) plus 100 mM NaCl and 2 mM DTT. The Smc1 head domain bound to Scc1-C was expressed in insect cells using the baculovirus system and purified as described[12].

Purified proteins were re-buffered into reaction buffer (25 mM NaPi pH 7.4, 50 mM NaCl, 10 mM $MgSO_4$, 0.25% Triton X-100) using a Superdex G-25 column, adjusted to 0.5 mg ml^{-1} and mixed quickly into one-twenty-fifth volume of DMSO, 5 mM bBBr (Sigma) or 25 mM BMOE (Pierce). Both crosslinkers were dissolved in DMSO just before use. After 10 min incubation at 4 °C, sample loading buffer containing β-mercaptoethanol was added, the samples were heated for 3 min at 90 °C and run on SDS–PAGE followed by Coomassie blue staining. Crosslinking reached a maximum after a few minutes at 4 °C (data not shown).

Yeast strains. All strains are derived from W303. Genotypes are listed in Supplementary Table 1.

Minichromosome preparation and crosslinking. Yeast strains containing the 2.3 kb minichromosome were grown, arrested in nocodazole and lysed by spheroplasting as described[7], with the exception that sodium citrate and sodium sulphite in the lysis buffer were replaced by 300 mM NaCl to increase minichromosome yield. Extracts were loaded onto an SW41 10–30% sucrose gradient in 25 mM HEPES-KOH pH 8.0, 50 mM KCl, 10 mM $MgSO_4$, 0.25% Triton X-100, 1 mM DTT, 1 mM PMSF. Gradients were run for 15 h at 18,000 r.p.m. and fractionated. Fraction aliquots were separated on a 1% agarose gel containing 0.5 μg ml^{-1} ethidium bromide as described[7]. Gels were transferred under alkaline conditions by capillary blotting onto Immobilon-NY$^+$ membrane (Millipore). The blots were hybridized with a ^{32}P-labelled probe for the 2.3 kb minichromosome sequence, exposed to imaging plates, scanned on an FLA-7000 image analyser (Fujifilm) and quantified using ImageQuant.

Minichromosome monomer or dimer peak fractions (~300 μl) were dialysed for 4 h against 500 ml reaction buffer at 4 °C in a Float-a-lyzer (SpectraPor) with a 100 kDa molecular mass cutoff. The dialysis buffer was replaced three times and then 24 μl of dialysed fraction was mixed quickly into 1 μl DMSO, 5 mM bBBr or 25 mM BMOE (both freshly dissolved in DMSO) and incubated at 4 °C for 10 min. Final concentrations of 200 μM bBBr or 1 mM BMOE were optimal for crosslinking (Supplementary Fig. 7). Bis-maleimide-based crosslinkers with longer spacers than BMOE, like BMB or BMH (Pierce), could be used with similar efficiency (data not shown). The reaction was quenched by the addition of 1.25 μl 210 mM DTT. For TEV cleavage, 24 μl of the quenched crosslinking reaction was mixed with 1 μl 5 mg ml^{-1} wild-type or C151A mutant TEV protease in TEV buffer (TEN buffer plus 50 mM NaCl and 2 mM DTT) or TEV buffer only and incubated at 30 °C for 1 h. Protein was denatured for 4 min at 65 °C after the addition of 2.8 μl 10% SDS. The denatured samples were mixed with 3 μl 80% sucrose containing 0.02% bromophenol blue and 20–25 μl of the mixture were loaded onto a 0.8% agarose gel containing 0.5 μg ml^{-1} ethidium bromide. Gels were run at 4 °C for 14 h at 1.4 V cm^{-1} and blotted and hybridized as before.

For two-dimensional gels, lanes from the first dimension agarose gels were cut out and placed at the top of a second 0.8% agarose gel (20 × 20 cm) containing 0.5 μg ml^{-1} ethidium bromide, leaving an approximately 5-mm-wide slot between the lane and the gel. The slot was filled with 60 °C warm 0.8% agarose in TAE. Proteinase K was dissolved in TAE and mixed with the pre-warmed agarose solution to a final concentration of 0.2 mg ml^{-1} just before casting. Second dimension gels were run at 4 °C for 8 h at 2 V cm^{-1}, blotted and hybridized as before.

For nicking minichromosome DNA, 200 μl crosslinked samples were first dialysed against 500 ml reaction buffer plus 2 M KCl and 1 mM DTT at 4 °C for 4 h to remove nucleosomes, then dialysed for 2 h against reaction buffer and 1 mM DTT to remove salt and finally dialysed for 2 h against reaction buffer with 20% sucrose and 1 mM DTT to re-concentrate the samples. Dialysis buffers were replaced every hour. One microlitre of Nb.BsrDI (10 U μl^{-1}) was added to 27 μl of sample followed by 10 min incubation at 50 °C, addition of SDS to 1% and denaturation as above.

Preparation of concatenated minichromosomes from a *top2* strain. Strain K15029 was grown at 23 °C to log phase in yeast synthetic drop-out medium without tryptophan (−TRP) plus 2% raffinose. Cultures were diluted to $A_{600\,nm} = 0.15$ and α-factor was added to a final concentration of 2 μg ml^{-1}. Additional α-factor was added to 1.5 μg ml^{-1} each after two 40 min intervals. Cells were collected by centrifugation and α-factor was removed by washing with four culture volume yeast extract peptone (YEP) plus 2% raffinose (YEPR) at 4 °C. Cells were resuspended in 35.5 °C warm YEPR containing 10 μg ml^{-1} nocodazole and grown for 1.5 h at 35.5 °C. Cells were collected and genomic DNA was prepared by spheroplasting as described above, with the exception that all steps including lysis were performed at 37 °C using buffers pre-warmed to 35.5 °C. Cleared lysates were loaded on pre-chilled 10%–30% sucrose gradients and processed as described above.

Centromere loop-out. Cells were inoculated into YEPR from an overnight culture in –TRP plus 2% raffinose and grown at 30 °C to $A_{600\,nm} = 0.6$. Galactose or glucose was added to a final concentration of 2%. The 30 min cultures were then diluted to $A_{600\,nm} = 0.15$ arrest with α-factor as described above. Cells were collected by centrifugation, washed with four culture volumes YEP plus 2% glucose (YEPD), resuspended in YEPD containing 10 μg ml^{-1} nocodazole and grown for 1.5 h at 30 °C. Genomic DNA was prepared as described in Supplementary Information and digested with EcoRI. Cleavage fragments were resolved on a 0.8% agarose gel, Southern blotted and probed for the *TRP1* gene.

Genomic DNA preparation. Yeast cells from 25–30 ml asynchronous culture were resuspended in 200 μl SCE (1 M sorbitol, 0.1 M sodium citrate pH 7.0, 60 mM EDTA) buffer plus 0.1 M β-mercaptoethanol and 1 mg ml^{-1} zymolyase T-100 and incubated for 1 h at 37 °C with occasional shaking. Spheroplasts were lysed by addition of 200 μl SDS lysis buffer (2% SDS, 0.1 M Tris-HCl pH 9.0, 50 mM EDTA) and incubated for 5 min at 65 °C followed by addition of 200 μl 5 M potassium acetate and centrifugation at 16,000*g* after 20 min incubation on ice. The supernatant (450 μl) was mixed with 1 ml isopropanol and 200 μl 5 M ammonium acetate, and precipitated genomic DNA was pelleted by 30 s centrifugation at 2,300*g*. All excess liquid was removed and the pellet was dissolved by 1 h incubation in 90 μl TE at 37 °C. Ten microlitre 5 M ammonium acetate and 200 μl isopropanol were added and genomic DNA was pelleted as above. The DNA pellet was washed with 1 ml 70% ethanol and dissolved in 50 μl TE containing 0.2 mg ml^{-1} RNase A. For restriction digests, 5 μl were used in a 20 μl reaction.

Purification of catalytically active and inactive TEV protease. Wild-type and catalytically inactive mutant (C151A) TEV protease[17] fused to an N-terminal His_6-tag were expressed from the pET9d vector in *E. coli* strain BL21(DE3)-RIPL (Stratagene) after induction with 0.25 mM IPTG for 6 h at 22 °C. Cells were lysed in 50 mM Tris-HCl pH 8.0, 1 mM β-mercaptoethanol, 1 mM PMSF. TEV protease was purified from the clarified extract using Ni^{2+}-chelating affinity chromatography and gel filtration on a Superdex 200 pg 26/60 column (GE Healthcare) in TEN buffer plus 50 mM NaCl and 2 mM DTT. TEV protease eluted as a single band at the expected delay volume and was concentrated to 5 mg ml^{-1} by ultrafiltration.

Testing cleavage of the Smc3–Scc1 linker. Protein extracts from 50 ml asynchronous cultures were prepared by glass bead lysis and the Smc3–Scc1 fusion protein was immunoprecipitated by its C-terminal HA_6-epitope tag with 16B12 antibody as described previously[6]. Immunoprecipitation beads were split and incubated in TEV buffer containing 0.1 mg ml^{-1} TEV protease or TEV buffer only for 2 h at 16 °C before addition of loading buffer, SDS–PAGE and western blotting. The blot was probed with 3F10 antibody (Roche) against the HA_6 epitope and exposed to film.

17. Hwang, D. C. *et al.* Characterization of active-site residues of the NIa protease from tobacco vein mottling virus. *Mol. Cell* **10,** 505–511 (2000).